4th International Conference on Silicon Photovoltaics, SiliconPV 2014

Passivation properties of subnanometer thin interfacial silicon oxide films

Wenjia Lu, Caspar Leendertz, Lars Korte, Jan Amaru Töfflinger, Heike Angermann

Institute Silicon Photovoltaics, Helmholtz Center Berlin, Kekuléstr. 5, 12489 Berlin, Germany

Abstract

Subnanometer thin silicon oxide films, applied as interlayer between crystalline silicon absorbers and functional layers, have demonstrated to improve interface passivation properties. Here we compare the interface defect density as well as the fixed charge of simple native air oxides to wet-chemical oxides on silicon substrates of different doping type, with different crystal orientations and after different chemical pre-treatment processes. We show that optimized wet-chemical pre-treatment and wet-chemical oxidation leads to strong improvement in terms of interface defect density as compared to simple oxidation in air. Furthermore we show that such subnanometer thin layers can contain large positive fixed charges of up to 10^{11} cm^{-2}. Due to excellently low defect densities for thin layers <0.5 nm, tunneling transport and thus application for solar cells with passivated contacts should be possible. While on p-type substrates such layers feature a high positive charge and would thus support an emitter band bending, on n-type substrates the charge is smaller and can even be negative due to electrons trapped in mid gap defects.

1. Introduction

In solar cell research one key issue is the design of passivation layers and layer stacks that provide a low interfacial density (D_{it}) of recombination-active defects and/or a high interface charge (Q_{it}) [1]. When applying conductive layers for interface passivation, the hetero offsets also play a major role for passivation, due to the fact that they separate the charge carriers from the highly recombination-active metal contacts. Lately an improvement of passivation quality of various passivation layer stacks has been achieved by introducing an additional subnanometer thin silicon oxide (SiO$_x$) layer at the silicon absorber surface. This concept has been applied in combination with dielectric passivation layer stacks based on silicon nitride and aluminum oxide [2-4]. Additionally such layers have

been applied in combination with conducting layers for the design of passivated contacts. Lately solar cells with a conversion efficiency of 21.8% featuring a passivated back contact based on an interfacial tunneling SiO_x layer in combination with highly doped polysilicon have been reported [4]. Furthermore a solar cell concept with passivated contacts based on an ultrathin SiO_x in combination with hydrogenated amorphous silicon (a-Si:H) layers has been proposed [5] and PV modules based on a similar concept are commercially available [6]. In such a silicon heterojunction solar cell the intrinsic amorphous silicon layers (a-Si:H(i)), which are typically used for interface passivation, are replaced by SiO_x as shown in Fig 1. It is expected that such solar cells lead to improved current due to reduced parasitic absorption in the SiO_x as compared to the intrinsic a-Si:H layer. Interestingly such SiO_x/a-Si:H(p,n) passivation stacks show similarly high charge carrier lifetimes as cells with a-Si:H(i)/a-Si:H(n,p) emitter and BSF. More specifically, the injection-dependent charge carrier lifetime curves show higher lifetime values at an injection level corresponding to the solar cell maximum power point while the lifetime at the injection level corresponding to open circuit conditions is slightly lower [5]. Such a difference in the shape of the lifetime curve indicates a different passivation mechanism, where the higher fixed charge in the thin SiO_x possibly contributes to the passivation [7].
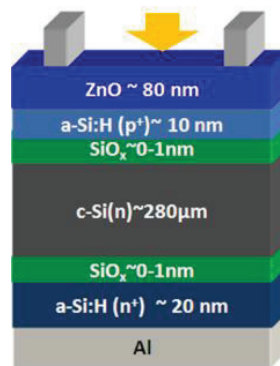

Fig. 1: Conventional silicon heterojunction solar cells can be modified by replacing the a-Si:H(i) layers with ultrathin SiO_x layers.

In this publication we determine the interface defect density and charge of different oxides with varying thickness by field-dependent photovoltage (SPV) measurements to understand the passivation mechanisms in detail. Since the interface properties of such layers strongly depend on the growth method and the substrate surface, we compare simple oxidation in air processing to oxidation in de-ionized water on silicon substrates of different doping types, with different crystal orientations and after different chemical pretreatment processes under technologically relevant conditions. While earlier publication have already discussed the defect density as function of the oxidation time on different surfaces in detail [8] we focus our investigations on the effective charge of such ultrathin layers and correlate defect density, charge and layer thickness. This is of special importance since the high charges that we determine in such subnanometer thin layers can strongly influence the band bending and thus a strong impact on solar cell characteristics must be expected. Therefore we finally discuss optimized layers for solar cell application in terms of layer thickness, defect density and fixed charge.

2. Experimental

2.1 Wet-chemical surface preparation

As substrate polished mono-crystalline n- and p-type silicon wafers (1-4 Ωcm) with (100) and (111) surface were investigated. The substrates were cleaned with the standard process established by the Radio Corporation of America (RCA) [9] which effectively removes particles as well as organic and metallic surface contamination. The remaining native oxides were etched in hydrofluoric acid solution (HF 1%) for 1 minute directly after RCA treatment in order to prepare oxide-free surfaces. To investigate the native oxide growth on HF-etched surfaces, a

set of Si(100) and Si(111) samples has been stored under clean-room air (25 °C, humidity about 50%) for up to two weeks. Since the wet-chemical preparation of ultra-thin passivating silicon oxide layers requires atomically flat, hydrogen (H) –terminated Si surfaces as starting point, the surface pre-treatment was specially optimized for Si(100) and Si(111) substrates as has previously been reported in [10]. A smoothing process is applied to reduce the micro-roughness of the sample surfaces. This smoothing process is based on the growth of a thin oxide in H_2O_2:HSO$_4$ (1:1) solution for 20 minutes. Subsequently the oxide is removed using (i) HF (1%, 1 min) for Si(100), or alternatively (ii) Ammonium fluoride solution (NH$_4$F 40%, 4.5 minutes) for Si(111) surfaces (see Fig 2). On the resulted smoothed and H-terminated surfaces, the wet-chemical oxides were prepared under clean-room conditions using de-ionized water of 18 MΩ resistivity (DiW) [11]. For oxidation the samples were immersed in DiW at a temperature of 80°C for 10 min up to 360 min immediately after the pre-cleaning procedure.
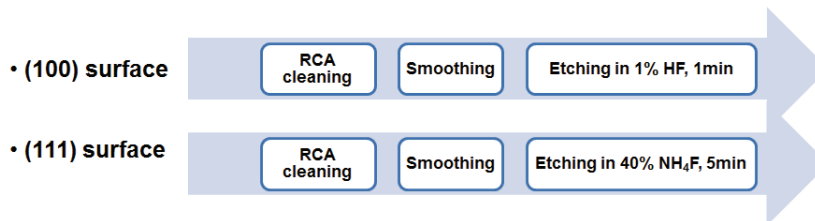

Fig. 2: Optimized process flow for chemical pre-treatment on different substrate surfaces

2.2 Surface characterisation methods

Two non-destructive and surface-sensitive spectroscopic characterization methods were employed in order to investigate the electronic interface properties of hydrogen (H)-terminated Si surfaces and of surfaces oxidized in clean-room atmosphere and in DiW.

The SPV technique was utilised to determine the fixed interface charge (Q_{it}) and the energy distribution of interface defect density ($D_{it}(E)$) as recently specified in [12]. This technique has the advantage that the measurements can be carried out directly after wet-chemical treatment without any contact preparation, using a mica foil as dielectric spacer. The sample is illuminated by a laser diode (902 nm, 150 ns pulse length) such that excess charge carriers are generated and a photovoltage is generated. The photovoltage can then be measured while varying the external voltages between a transparent electrode and the wafer. To minimize the effects due to charge accumulation each field voltage pulse of 100 ms is followed by an inverted but otherwise identical pulse [13]. By recording the SPV signal without the external voltage the surface band-bending can be determined, from which Q_{it} can be calculated. By measuring the surface band bending as function of an external voltage U_F, the defect density $D_{it}(E)$ can be obtained [12]. This method to determine $D_{it}(E)$ was first described 1968 by Heilig [14].

Ex-situ spectroscopic ellipsometry (SE) in the ultraviolet and visible (UV-VIS) spectral range was utilised to determine the surface roughness immediately after preparation. This effective thickness $<d_r>$ will be denoted as "micro-roughness" in the following. Furthermore the effective oxide layer thickness $<d_{ox}>$ was determined directly after each oxidation step. For determination of those effective thicknesses three angle measurements were performed at the angles of incidence of 70°, 60° and 50° in the wavelength range of 250 nm to 800 nm. Since the imaginary part of the pseudo-dielectric function at the E_2 silicon critical point is near 4.25 eV, the low wavelength region is of highest sensitivity to surface modifications and thin layers [15]. This wavelength range is sensitive to a thickness change in the subnanometer range such that the micro-roughness $<d_r>$ and the effective thickness of the native oxide $<d_{ox}>$, respectively, can be obtained by a data fitting routine. For data fitting a three-layer model was used that consists of bulk c-Si, a Bruggeman effective medium [16] layer consisting of 50 % bulk c-Si and 50 % SiO$_2$ to describe the micro-roughness and a SiO$_2$ layer. Directly after surface treatment the thickness of the Bruggeman layer was determined and after oxidation the thickness of SiO$_2$ layer was calculated assuming a fixed micro-roughness thickness.

3. Results

3.1 Micro-roughness and defect density for optimized chemical pre-treatment

Fig. 3 shows interface state distributions $D_{it}(E)$ calculated from field-depended SPV measurements on a) Si(100) and b) Si(111) samples. The samples were smoothed and H-terminated by the $H_2O_2:HSO_4$ (1:1) treatment followed by HF and NH_4F treatment, respectively. The U-shaped energetic distribution of rechargeable interface states can be separated into two groups of intrinsic states resulting from strained ($Si_3\equiv Si$—$Si\equiv Si_3$) bonds and from dangling bond defects back bonded only to silicon ($Si_3\equiv Si-$). The defect group around mid gap has been identified by EPR measurements in earlier investigations [17]. On Si(111)/SiO$_2$ interfaces, the analogous defect has been identified mainly as an unpaired *sp3* orbital on a trivalently bonded interface Si atom or Si(111)-oriented Si dangling bond pointing out of the interface into the oxide [18]. The two related defects on the Si(100)/SiO$_2$ and Si(111)/SiO$_2$ interface are denoted as P_{b0} and P_b, respectively.

The minimum defect denity $D_{it,min}$ of the U-shaped energetic interface states distribution $D_{it}(E)$ is chosen here as a measure for the electronic quality of wafer surfaces and interfaces in the technological process. Since the saturation of dangling bonds by hydrogen eliminates surface states, very low minimal values $D_{it,min}$ can be achieved on carefully prepared H-terminated surfaces. On H-terminated Si(111) surfaces prepared by NH_4F treatment, the lowest $D_{it,min} < 4 \times 10^{11}$ cm^{-2}eV^{-1} and surface micro-roughness $<d_r> \cong 1$ Å (Tab. 1) were achieved. On Si(100) surfaces, higher values of $D_{it,min} > 5 \times 10^{11}$ cm^{-2}eV^{-1} and narrower U-shaped energetic distributions (Fig. 3a curve 2) and as well as higher surface micro-roughness ($<d_r> \geq 4$ Å) (Tab. 1) were observed.
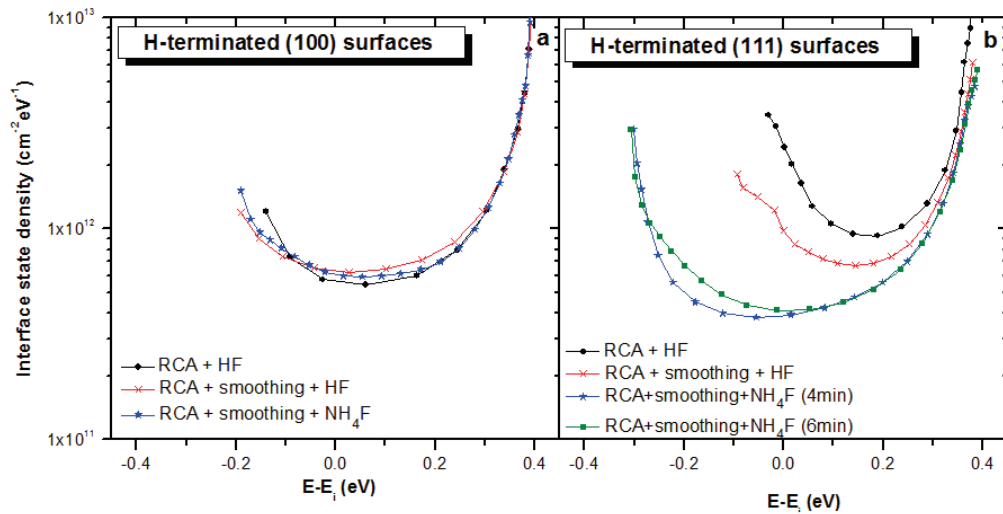

Fig. 3: Energetic distributions of interface states $D_{it}(E)$ of H-terminated n-type Si(100) (a) and Si(111) (b) surfaces after wet-chemical smoothing and treatment with HF (1%, 1 min) and NH_4 (40%) solutions, respective

Table. 1: Micro-roughness (MR) and $D_{it,min}$ of H-terminated n-type Si(100) and Si(111) and p-Si(111) substrates after different etching methods

	(100) surface (n-type)		(111) surface (n-type)		(100) surface (p-type)	
	MR (nm)	D_{it} $(10^{11}cm^{-2}eV^{-1})$	MR (nm)	D_{it} $(10^{11}cm^{-2}eV^{-1})$	MR (nm)	D_{it} $(10^{11}cm^{-2}eV^{-1})$
HF (1% 1 min)	0.4	5.4	0.3	9.2	0.4	4.7
HF (1% 1 min) +smoothing	0.4	6.2	0.3	6.7	0.4	4.6
NH₄F (40% 4.5 min)+smoothing	0.4	5.9	0.1	3.8	0.4	7.5

3.2 Native and wet-chemical oxide growth on H-terminated Si(100) and Si(111) surfaces

Simultaneous SPV, UV-VIS SE measurements were performed to monitor the change of the electronic surface properties during oxide growth as function of the oxide thickness. The increasing effective oxide thicknesses $<d_{ox}>$ as function of the oxidation time was derived from ellipsometric measurements on n- and p-type Si(111)- and Si(100)-samples. Fig. 4a shows the evolution of $<d_{ox}>$ during storage in clean room air and Fig. 4b,c during immersion in DiW at 80°C. The oxide growth velocity strongly depends on the oxidation method and the surface orientation, while the substrate type has a minor influence. The oxidation in clean room air on a RCA cleaned and HF dipped sample on (100) surface is comparably slow and the oxide thickness exceeds $<d_{ox}>$ =1 nm only after approximately 7 days (Fig. 4a). The wet-chemical oxidation in DiW at 80° C saturates already after approximately 5 hours. The Si(100) oxidizes faster and reaches $<d_{ox}>$ =1 nm thickness already after 10 – 30 min while on Si(111) this thickness is still not reached until 100 – 300 min (Fig. 4b,c). The final effective oxide thickness is approximately $<d_{ox}>$ =1 nm on Si(111) and $<d_{ox}>$ =4 nm on Si(100) substrates, respectively.

The corresponding interface state distributions $D_{it}(E)$ as obtained by SPV measurements on nominally identical, n-type Si(111) and Si(100) samples after oxidation in air are shown in Fig. 4d and after wet-chemical oxidation in DiW in Fig. 4e,f. The oxidation in air leads to a higher $D_{it,min} > 10^{12}$ cm^{-2}eV^{-1} and significantly narrower U-shaped energetic defect distributions. This is attributed to the higher surface micro-roughness and un-stoichiometric oxides SiO$_x$ (Fig. 4d). To avoid both, irregular native oxide growth and contaminations, the preparation of thin passivating oxide layers in hot water was performed under clean room conditions immediately after optimized chemical surface pre-treatment. The final interface state densities $D_{it,min} < 5 \times 10^{11}$eV^{-1}cm^{-2} (Fig. 4e,f) of the resulting thin oxide layers on (111) and (100) surfaces are clearly superior since the U-shaped defect densities $D_{it}(E)$ are lower and wider than that of conventionally prepared oxides in the thickness range of 1 to 2 nm. We assume that the layer-by-layer oxide growth on the atomically flat H-terminated surface leads to lower defect densities due to a well-ordered interface during the formation of the first monolayers. Comparing the wet-chemical oxides on different surfaces it can be observed that the defect density on (100) surfaces is slightly lower, but the width of the measured defect distribution is also narrower than on (111) surfaces. Furthermore it can be observed that defects above and below the intrinsic Fermi level E_i (compare dashed lines in 4e,f) change differently with oxidation time and oxide thickness, respectively. This behavior has been investigated earlier and it is explained by dangling bond defects leading to defect densities that can be described by Gaussian distributions at different energetic positions in the band gap, which are typically denoted as P_{b0} and P_{b1} states. The difference between the (100) and (111) surface and the variation of the different dangling bond states with oxide thicknesses has been discussed in detail earlier [10]. In this publication we focus our attention on the interface charge and the impact of defect states on the charge state of the interface.
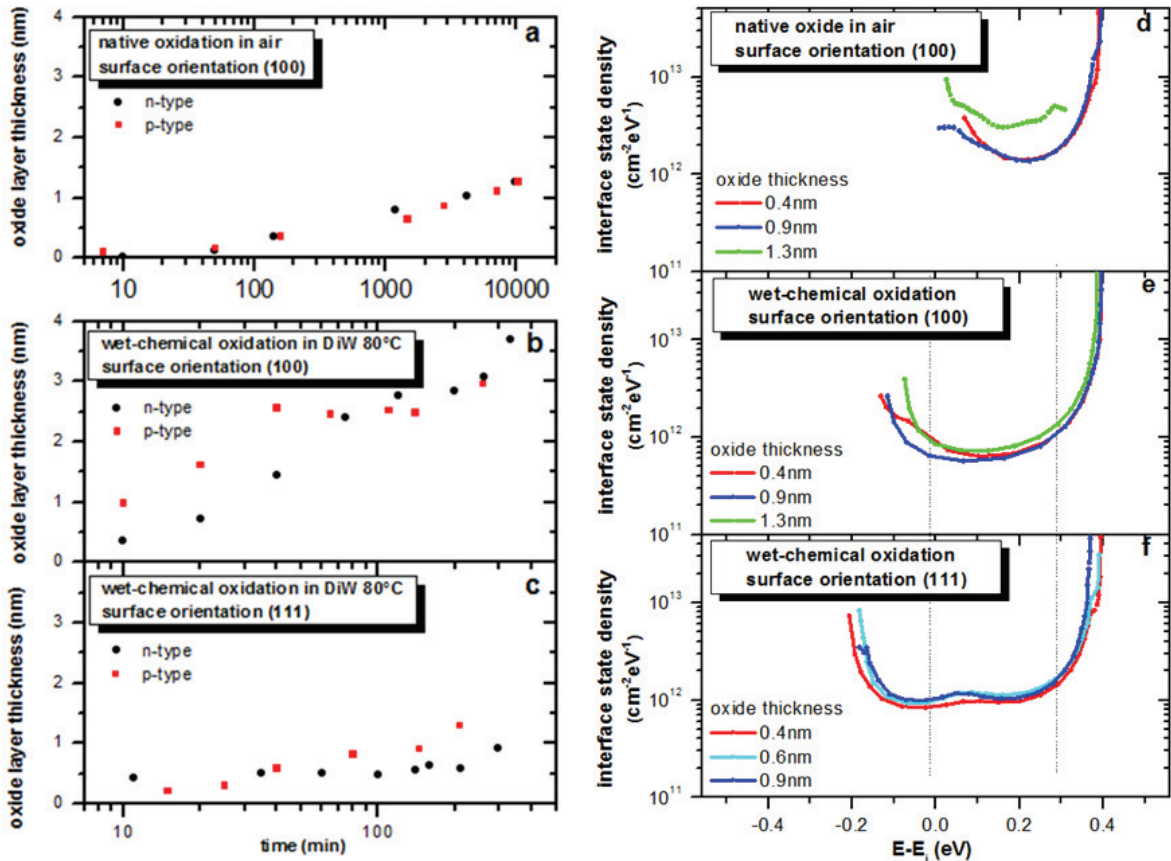
Fig. 4: Effective oxide thickness as function of the oxidation time determined with UV-VIS SE for the oxidation in air (a) and the oxidation in DiW (b,c) for different wafer types and surface orientations. Defect state density as function of the band gap energy as obtained from field-dependent SPV for the oxidation in air (d) and the oxidation in DiW (e,f) for different wafer types and surface orientations

In Fig. 5a the minimum defect density $D_{it, min}$ and in Fig. 5b the corresponding effective charge for oxidation in air on n-type and p-type substrates with (100) surfaces are shown as functions of the oxide thickness. The defect density increases with the oxide thickness similarly on n-type and p-type substrates. However the effective interface charge shows a different signature. For p-type substrates a high positive charge of 2×10^{11} cm^{-2} can be found that decreases with oxide thickness, while on n-type substrates a smaller charge is observed that decreases more strongly and becomes even negative. In Fig. 5c the effective charge is shown as function of the minimum defect density and a clear correlation can be found. Thus it becomes evident that the variation in charge can be explained by electrons trapped in mid gap defects. For n-type substrates more defects lie below the Fermi level and thus the negative charge will increase strongly with defect density while this effect is not as strong on p-type since the Fermi level lies closer to mid gap.
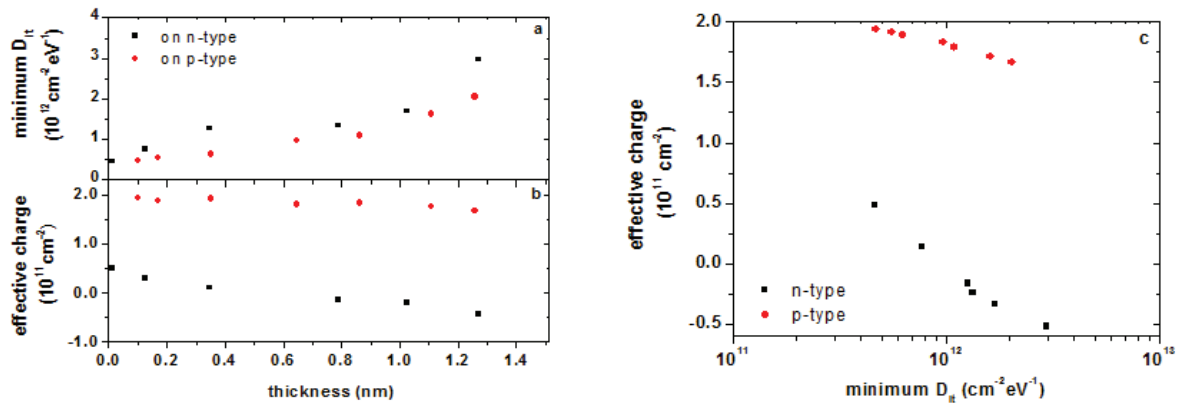
Fig. 5: Minimum defect density $D_{it, min}$ (a) and effective charge (b) for oxidation in air on n-type and p-type substrates with (100) surfaces as functions of the oxide thickness and effective charge plotted as function of the minimum $D_{it,min}$ (c).

In Figure 6a the effective charge of wet-chemical oxides is shown as function of the oxide thickness. As in the case of native air oxides the charge on p-type substrates is positive and high values of 10^{11} cm^{-2} are reached while on n-type substrates the charge is smaller and negative. However in the case of wet-chemical oxides no clear correlation between defect density and effective charge can be found. It can be assumed that similar mechanisms of electron trapping in mid gap dangling bond defects are responsible for the difference in charges on n-type and p-type substrates. However the detailed understanding is complicated due to the fact that the defect density does not increase over the whole band gap but separate defect peaks at different energy positions shift separately as can be seen in Fig. 4e,f.
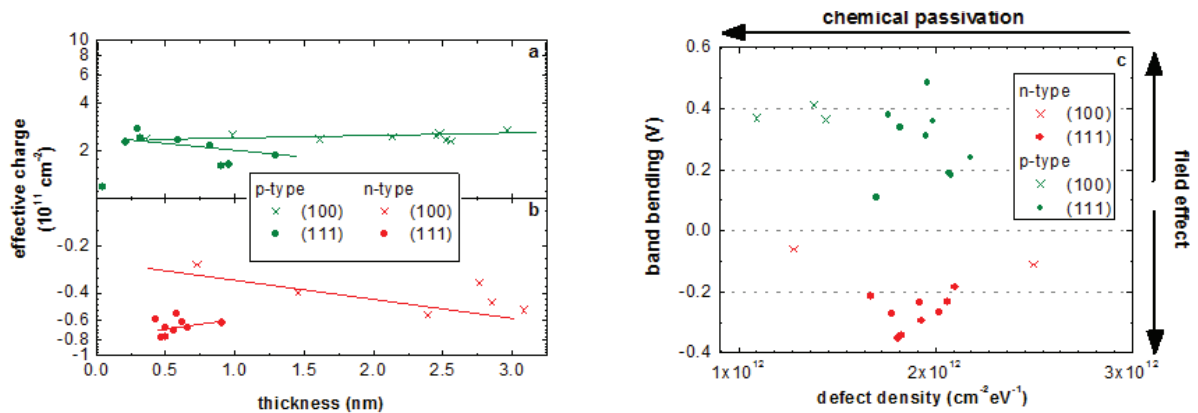

Fig. 6: Defect density $D_{it, min}$ at energy positions (E-Ei=-0.1eV) and (E-Ei=+0.2eV) and effective charge Q_{eff} for wet-chemical oxides on n-type and p-type substrates with (100) and (111) surfaces as functions of the oxide thickness. The lines are guides for the eye.

Finally the implications for solar cell applications are summarized in Fig. 6b. This figure shows the band bending that is induced by such layers due to their effective charge as function of the defect density. Only the wet-chemical oxides are shown in Fig 6b since they are superior in terms of interface defect density as compared to native air oxides. Furthermore only layers with thicknesses <2 nm are shown such that tunnelling transport and an application as passivating, tunnelling layer is possible. It can be seen that on p-type wafers the lowest defect density is obtained on (100) surface and that such layers induce a positive band bending. Thus on p-type substrates such layers would support emitter band bending and are well suited for the application at the solar cell front side. On n-type substrates

the lowest defect density is also obtained on (100). However the band bending is comparably small and thus such layers can neither improve emitter nor back surface field band bending.

4. Conclusions

In this study the interface defect density as well as the fixed charge of simple native air oxides has been compared to wet-chemical oxides on silicon substrates of different doping types, with different crystal orientations and after different chemical pretreatment processes. We have shown that wet-chemical oxides are more suitable for interface passivation due to very low and broad defect distributions. Furthermore both types of oxides show a fixed charge of about $+2x10^{11}$ cm^{-2} on p-type substrates while the fixed charge on n-type substrates is smaller and can be even negative. Native air oxides show a clear correlation between Q_{it} and D_{it}, which can be explained by electron trapping in mid gap defects. The correlation between Q_{it} and D_{it} for wet-chemical oxides is more complicated and a more precise measurement of $D_{it}(E)$ would be necessary for detailed understanding. For application in solar cells wet-chemical oxides on p-type (100) and n-type (100) substrates are most suitable due to low $D_{it}s \approx 10^{12}$ cm^{-2}eV^{-1}. On p-type substrates such layers have a high positive $Q_{it} \approx +10^{11}$ cm^{-2} and would support the emitter band bending. On n-type substrates the charge is negligible for low D_{it} and therefore such layers can be applied for chemical interface passivation at the emitter or the back surface field side of a solar cell.

Acknowledgements

References

[1] Aberle, A. G., Prog. Photovoltaics Res. Appl. 8, 473–487 (2000).
[2] Chowdhury, et al. Appl. Phys. Lett. 101, 021601 (2012).
[3] Laades, A. et al., Solid State Phenom. 195, 310–313 (2012).
[4] Feldmann, F., et al., Sol. Energy Mater. Sol. Cells 120, 270–274 (2013).
[5] Varache, R. ,et al., in 27th Eur. Photovolt. Sol. Energy Conf. Exhib. 1582–1585 (2012).
[6] J. Fu, et al. ,in 28th Eur. Photovolt. Sol. Energy Conf. Exhib. Poster Present. Paris, France, (2013).
[7] Leendertz, C., et al. Appl. Phys. Lett. 98, 202108 (2011)
[8] Angermann, H., et al. Sol. En. Mat. Sol. Cells, 83, 331–346 (2004).
[9] Kern, W., J. Electrochem. Soc. 137(6), 1887-1892 (1990).
[10] Angermann, H., et al. Mater. Sci. and Eng. B73, 178-183 (2000).
[11] Angermann, H., et al. Appl. Surf. Sci. 235, 322-339 (2004).
[12] Angermann, H., et al. Appl. Surf. Sci. 254, 8067-8074 (2008).
[13] Heilig, K., Solid State Electron. 27(4), 395 (1984).
[14] Hellig, K., Exper. Techn. Der Phys. 14, 135 (1968).
[15] Aspnes, D.E., et al. Sci. Technol. 18, 289 (1981).
[16] Bruggeman, D.A.G., Ann. Phys. (Leipzig) 24, 636 (1935).
[17] Pointdexter, E.H., Appl. Phys. 56, 2844 (1984).
[18] Pointdexter, E.H., et al. Appl. Phys. 52, 879 (1981).